J Mater Sci (2008) 43:1630–1637
DOI 10.1007/s10853-007-2296-0

Propene/1-octene copolymers as a new pervaporative membrane material for wastewater treatment

Xiuzhi Tian · Xue Jiang

Received: 2 May 2007 / Accepted: 2 November 2007 / Published online: 25 December 2007

Abstract Organophilic pervaporation is an interesting and promising membrane technology for wastewater treatment, and its topic is always to develop new membrane materials with high separation and application properties. In this study, a new polymeric membrane material-propene/1-octene copolymers (P-*co*-Os) were synthesized by means of slurry polymerization process under atmospheric pressure using Ziegler–Natta catalyst ($MgCl_2/TiCl_4/AlEt_3$). The aim was to investigate the correlation between the copolymeric structures and properties. Results from copolymerization showed that at 50 °C, when the mole ratio of Al in $AlEt_3$ and Ti in $TiCl_4$ was 100 and 1-octene concentration was over 0.168 mol/L, random and low-crystalline P-*co*-Os were obtained. They were demonstrated to have excellent thermal stability and higher mechanical strength than the generally used PDMS membrane. P-*co*-Os with about 24.6 mol% 1-octene content, its weight loss started at about 400 °C and break strength was 1.7 MPa. Moreover, from pervaporation measurements with chloroform/water mixtures, it was found that an increase of 1-octene content in P-*co*-Os resulted in a decrease of glass transition temperature (T_g), and thus the higher permeate flux but lower selectivity appeared. In general, P-*co*-Os did exhibit prospects for organophilic pervaporation.

X. Tian (✉) · X. Jiang
School of Textiles & Clothing, Key Laboratory of Eco-Textile, Ministry of Education, Jiangnan University, Wuxi 214122, China
e-mail: xzhtian@yahoo.com.cn

Introduction

Water contamination by volatile organic compounds (VOCs), such as chloroform, which is encountered in several chemical industries, groundwater and site remediation applications, is a major environmental and economical problem. For the separation of VOCs from aqueous solution, organophilic pervaporation (O-PV) in particular is regarded as an interesting alterative to conventional processes such as distillation, extraction, adsorption or stripping [1–4]. The selectivity of pervaporation is based on the differences in sorption and diffusion behavior of the feed components. The achievement of separation results from the differences in permeation velocities of the permeating components [5–8].

The polymeric membrane is the heart of O-PV. It can be considered as a dense homogenous medium in which diffusion of species takes place in the free volume that is present between the macromolecular chains of the polymeric membrane material. So far, only a few polymers or copolymers have been adopted in O-PV. Polydimethylsiloxanes (PDMS), poly(ether-block-amide) (PEBA), polyurethane (PUR), ethylene propene diene monomer rubber (EPDM), polyvinylidene fluorine (PVDF), etc., were reported to be typical polymeric materials for O-PV [9]. One of the reasons for this lack of efficient membrane material is that the selective removal of organic compounds dissolved in water is always a challenge due to the diffusion property of water: indeed water is known to be a fast molecule compared to organic ones whatever the type of polymers used in pervaporation, i.e. rubbery or glass ones.

Membrane is the heart of an O-PV process. So the choice of membrane material for O-PV is very important. From the solubility point of view, strong hydrophobicity is necessary to increase repellence for water and affinity for VOCs. In addition, from the diffusivity point of view, an

increase of the free volume is needed in order to reduce the difference of diffusing rate between water and VOCs [10–13].

Polyolefins seem to be potentially ideal membrane materials for O-PV in consideration of their high hydrophobicity. Nevertheless, homopolyolefins, such as polypropene, cannot be used directly in O-PV because their crystals will induce large diffusion resistance. In this regard, reducing the crystallinities of homopolyolefins should be an effective way to obtain new O-PV membrane material. And copolymerization is an effective way to obtain polyolefins with low crystallinities or large free volume. In this regard, α-olefin can be chosen to be copolymerized with propene because of its long chain [14]. In our previous work, propene/1-decene copolymers (P-*co*-Ds) were successfully synthesized and applied as the pervaporative membrane material for chloroform/water separation [15].

In this article, 1-octene as another α-olefin was chosen to be copolymerized with propene, and the obtained copolymers (P-*co*-Os) were firstly reported to be used in O-PV of chloroform/water mixtures. Moreover, the correlation between their structural parameters, which were characterized by FT-IR, ^{13}C NMR, wide-angle X-ray diffraction (WAXD), DSC and the pervaporative separating performances, was primarily investigated.

Experimental procedure

Materials

1-Octene, 98 wt.% purity, was purchased from Sigma–Aldrich. Triethyl aluminum ($AlEt_3$) was procured from Aldrich. The DQ-1 Ziegler–Natta catalyst (red-brown spheric powder) was supplied by Sinopec Beijing Research Institute of Chemical Industry. Petroleum ether and diphenyl dimethylsiloxane (DPDMS) were obtained from Hubei Institute of Chemical Engineering, China. Isopropanol, *n*-hexane, anhydrous ethanol, hydrochloric acid and chloroform were of reagent grade (99% pure) and were used without further purification. Polyester (PET) supported poly(vinylidene fluoride) (PVDF) substrates were supplied by the National Center of Ocean Water Treatment, Hangzhou, China.

Copolymerization

1-Octene was refluxed over Na, distilled and stored over calcium hydride under argon. Petroleum ether was refluxed over Na before using. Propene/1-octene copolymerization was conducted in a 250-mL Schlenk flask at 50 °C in a water bath with magnetic stirring. During the overall reaction, an atmosphere of propene was maintained above the solution at a given pressure (1.026×10^5 Pa). Firstly, polymerization grade propene was purified by passing through a series of three self-made absorption towers composed of desulfurator, deoxidizer and molecular sieve to remove residual traces of sulfur, oxygen and moisture, respectively, and was passed into the flask continuously. Next, petroleum ether, 1-octene, $AlEt_3$, DPDMS were introduce into the reactor, and the solution was stirred for 5 min to ensure uniform mixing before the polymerization started as soon as the catalyst was added. After the polymerization was continued for 1 h, a mixed solution of ethanol, isopropanol with a volumetric ratio of 1:1 containing 0.5 vol.% hydrochloric acid was added into the reaction flask to stop the polymerization. The obtained copolymers were extracted by using an 100 mL Soxhlet's apparatus with *n*-hexane for several times. Every extraction was kept on for 24 h. The n-hexane-soluble copolymers were precipitated into rubber-like solids with isopropanol. Finally, the products were vacuum-dried at 50 °C for 48 h, and were used for characterization and membrane fabrication [16].

The mole ratio of Al in $AlEt_3$ and Ti in $TiCl_4$ was 100. The apparatus used in copolymerization is shown schematically in Fig. 1.

Characterization of copolymers

^{13}C NMR spectra of P-*co*-Os were obtained on a Bruker AMX400 NMR spectrometer to analyze the composition and sequence distribution of the copolymers. *o*-Dichlorobenzene-d_4 was used as solvent and hexamethyldisiloxane

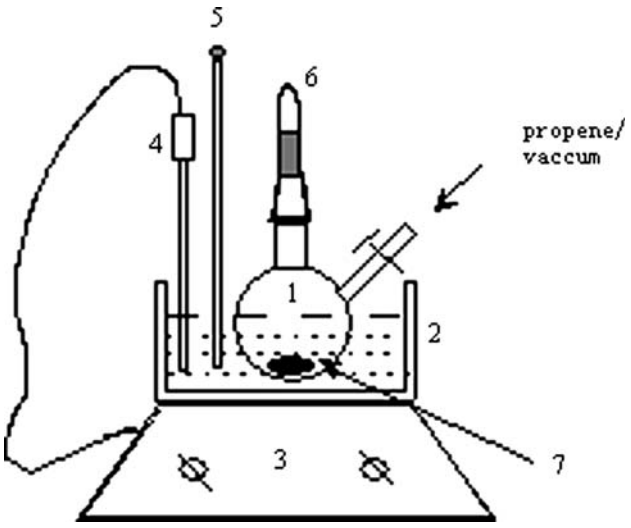

Fig. 1 Propene/1-octene copolymerization apparatus. (1) Schlenck flask; (2) water bath; (3) heater and magnetic stirrer; (4) temperature sensor; (5) thermometer; (6) catalyst container; (7) rotator

as the internal standard. FT-IR spectra were obtained using a Bruker Vector 22 type spectrometer. WAXD patterns were recorded with an X-Ray Diffractometer (XD-98, Philips). Calorimetric analysis (weight loss) was carried out in a TA® SDT Q100 calorimeter at a heating rate of 10 °C/min from 25 to 600 °C. A TA® SDT Q600 analyzing system connected to a cooling system and different standards were used to calibrate the glass transition temperature (T_g). The temperature was gradually increased from −100 to 150 °C. Break strength of the fabricated membrane was tested on an AG-1 (Japan) electronic serimeter.

Membrane preparation and characterization

PVDF/PET-supporting membrane was fixed on a glass plate and coated with 4 wt.% *n*-hexane-dissolved copolymer solution. P-*co*-Os coated PVDF/PET composite membranes were obtained by evaporating *n*-hexane in the air [17]. A field emission scanning electron microscope, Hitachi® S-520 was employed to view the membrane morphology. The membrane thickness was measured using an electronic gauge in combination of the SEM photograph. Ten separate thickness measurements were taken at equal spacing around the circumference of the membrane and the average value was used. The skin layer of the composite membrane was about 5 μm.

Pervaporation experiments

A traditional pervaporation apparatus was used in this study [18]. The circular flat membrane was clamped into a sealed stainless steel test cell above a porous sintered metal support with a 'o' ring arrangement forming a leak free seal, giving a pervaporation area of 28.26 cm^2. The cell was filled with the feed solution and stirred at 16.66 Hz (1,000 rpm) by a magnetic agitator. The cell temperature was controlled and measured with a thermocouple and electronic temperature control system, accurate to 25 ± 0.5 °C. A vacuum pump maintained the downstream pressure at 300–400 Pa. The permeate was condensed and frozen with the cold trap, which was cooled with liquid nitrogen. The permeation rate was determined by measuring the weight of the permeate. The compositions of the feed solution and permeate were measured by gas chromatography (GC, China Chromatography 120).

Permeate flux, J (g m^{-2} h^{-1}), was calculated using the expression [17]:

$$J = \frac{Q}{AT} \tag{1}$$

where Q (g) was the total amount of permeate passed through the membrane during an experimental time interval T (h) at a steady state and A (m^2) was the effective area of the membrane.

The separation factor was calculated from the following equation [17]:

$$\alpha_{CHCl_3/H_2O} = \frac{Y_{CHCl_3}/Y_{H_2O}}{X_{CHCl_3}/X_{H_2O}} \tag{2}$$

where Y_{CHCl_3} and X_{CHCl_3} were the weight fractions of chloroform in permeate and feed, respectively, and Y_{H_2O}, X_{H_2O} were the weight fractions of water in permeate and feed, respectively.

Results and discussion

Characterization of P-*co*-Os

A series of P-*co*-Os were synthesized by means of slurry polymerization process under atmospheric pressure with different 1-octene concentration using Ziegler–Natta catalyst ($MgCl_2/TiCl_4$). With a given catalyst system, the length of the branches and the co-monomer content are important parameters for elucidating the chain configuration and the ultimate crystallinity of the copolymer and therefore, its macroscopic properties, containing the pervaporative separating properties of its membrane [19]. In this article, the co-monomer content (or the composition), the binary sequence distribution of P-*co*-Os and the average sequence lengths of propene and 1-octene were determined by analysis from ^{13}C NMR spectra. Results were listed in Table 1 and Fig. 3. Assignment of carbon atoms can be seen in Fig. 2 and calculation of chemical shift values can be referred to Grant and Paul [20].

Table 1 shows that P-*co*-Os with different 1-octene contents were obtained with this versatile catalyst system, proving its prospects for tailoring olefin copolymers with targeted properties.

The binary sequence distribution of P-*co*-Os with different compositions as presented in Table 1 indicates that

Table 1 The compositions and binary sequence distribution of the synthesized P-*co*-Os

P-*co*-Os sample	1-Octene content in P-*co*-Os (mol%)	Composition of binary sequence			$\frac{[PO]}{[PO]+[OO]}$
		PP	*PO*	*OO*	
a	5.3	0.891	0.089	0.020	0.817
b	16.4	0.692	0.272	0.036	0.883
c	19.1	0.636	0.303	0.061	0.832
d	24.6	0.557	0.363	0.090	0.801

Note: *PP*, *PO*, *OO* denote the binary sequence; [*PO*], [*OO*] are the ratio of *PO*, *OO* in the total binary sequences, respectively

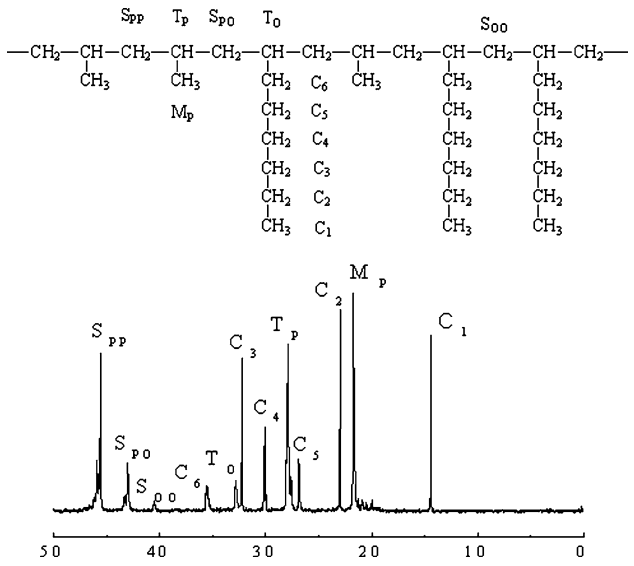

Fig. 2 ^{13}C NMR spectrum and peak assignment of P-*co*-Os. M, S, T denote the kind of carbon atoms in the main macromolecular chains which are methyl, methylene and methyne group, respectively; the subscripts denote the origin of the third class carbon atoms which are on the left and on the right of the methylene respectively; P is propene and O is 1-octene

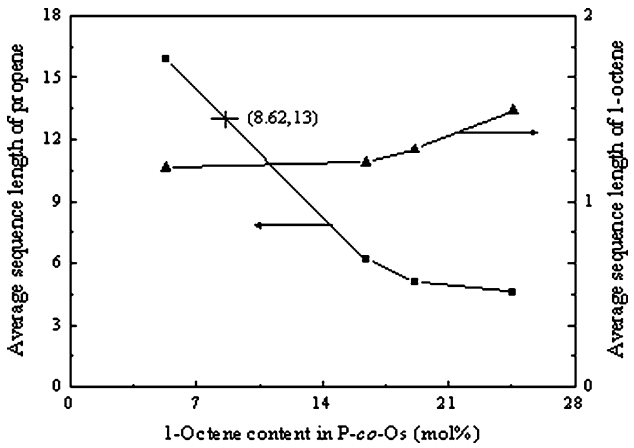

Fig. 3 Effect of 1-octene content in P-*co*-Os on the average sequence lengths of propene and that of 1-octene

1-octene is incorporated randomly in the copolymers. Furthermore, for each P-*co*-Os, the content of *OO* is very low, whereas the ratio of *PO* in all of the binary sequences including 1-octene unit (*PO* and *OO*) is more than 80%. Consequently, it can be inferred that 1-octene in the copolymeric backbone chains is mainly inlaid as an individual unit and the chain structures of the obtained copolymers are somewhat comb-like. In brief, in addition to the space among the branches, the relatively long branches keep the polymeric chains apart, creating more space between macromolecular chains, which in a microscopic scale means a larger free volume. At the same time, the introduction of relatively long 1-octene branches will reduce the crystalline size and crystallinity in the copolymer, which can be further verified by FT-IR and WAXD analysis.

In fact, the analyzing results from the average sequence length is consistent with that from the binary sequence distribution. Table 1 shows that with an increase of 1-octene content in P-*co*-Os, the content of *PP* exhibits an obvious decreasing trend, but that of *OO*, *PO* increase instead, which implies that when propene is copolymerized with 1-octene, the regulation of the backbone chain of polypropene is destroyed by the relatively long branches of 1-octene. Hence, the average sequence length of propene is reduced, as presented in Fig. 3, and it decreases with increasing the 1-octene content in P-*co*-Os. In this regard, it is not difficult to predict that the according crystallinities of copolymers are thus evidently decreased.

Figure 3 also shows that the average sequence length of 1-octene is only between 1 and 2. On the one hand, it accounts for the crystallinities of P-*co*-Os being only related to the chain segments of propene. On the other hand, it demonstrates that no homopolyoctene is admixed in the obtained copolymerization products. This is important for olefin copolymerization because relatively pure copolymers (P-*co*-Os) are easy to be separated from the products.

Moreover, as seen from Fig. 3, when 1-octene content in P-*co*-Os is over 8.62 mol%, the average sequence length of propene is about 5–13. Chain segments with such a length are difficult to form crystals [21]. Moreover, according to Fig. 4, which presents the correlation between the 1-octene reactive concentration and the composition of P-*co*-Os, it can be noted that under the condition employed in this article during propene/1-octene copolymerization and when

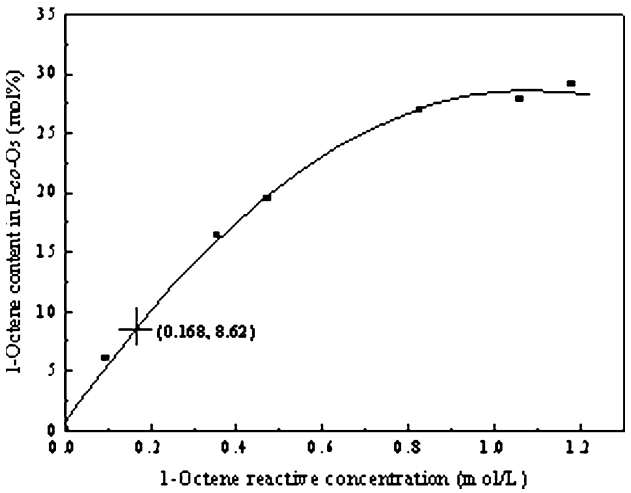

Fig. 4 The correlation between the 1-octene reactive concentration and the composition of the obtained P-*co*-Os. The pressure of propene is 1.026×10^5 Pa and mean yield of copolymerization is 7 kg-polymer/(g Ti h)

1-octene concentration is controlled over 0.168 mol/L, the average sequence length of propene in the obtained P-*co*-Os will not exceed 13, that is, the obtained P-*co*-Os do bear very low crystallinities.

The configurations of the products from propene/1-octene copolymerization are shown in Fig. 5. It can be seen that substances like cobweb increase with an increase of the 1-octene concentration during copolymerization, which explains that they are just the products of P-*co*-Os.

Figure 6 shows the WAXD patterns of P-*co*-Os with different 1-octene contents. The main peaks in curve a with 2θ at 14°, 17°, 19°, 21°, 29°, 43° demonstrate that P-*co*-Os should have X-ray detectable crystalline characteristic of homopolypropene. This observation is in agreement with the sequence length analysis from ^{13}C NMR spectrum.

Figure 6 also shows that the amount of the crystalline polypropene visible in the WAXD patterns decreases with increasing the 1-octene content in P-*co*-Os and becomes lost in the background when the 1-octene content increases to some extent. Increasing amounts of 1-octene incorporated into the copolymers will gradually disrupt the crystalline structure, since the relatively long branches will impart defects to the polymeric chains, creating obstacles for the organization of crystalline region. Actually, weak peak intensity in Fig. 6 reflects that the crystallinities of all the synthesized P-*co*-Os are very low and crystals are likely to exist in crystallites. Whatever, the diffusive curves of the copolymers indicate that they are nearly amorphous.

Figure 7 is the FT-IR spectra of P-*co*-Os with different compositions. Among those bands, the ones at 720 and 1,150 cm^{-1} are representative of the 1-octene and propene units in copolymers, respectively. From Fig. 7, it can be seen that the proportion of band intensity between 1-octene and propene units does increase with an increase of the 1-octene content in P-*co*-Os.

It is known that 998 cm^{-1} is related to the long propene chain segments with its number of repeated unit over 11–13. Chain segments with such a length can form crystals. Besides, 975 cm^{-1} is related to the relatively short chain segments of propene, which appears when its number of repeated unit is more than 5 [21]. Chain segments with such a length are difficult to form crystals. As seen from the curves of samples a–d in Fig. 7, both the band at 998 cm^{-1} and that at 975 cm^{-1} appear. But great disparity of the band intensities does exist between 998 and 975 cm^{-1}, which demonstrates again that the crystallinities of the obtained P-*co*-Os are positively low.

It is well known that the mechanical strength of the relative material will be weaken with a decrease of its crystallinity. The break strength of sample d with highest 1-octene content is about 1.7 MPa. It is higher than that of PDMS (0.2–0.3 MPa) [22]. It illuminates indirectly that the crystallites existing in P-*co*-Os act as the cross-linking points and confine the mobility of the amorphous phase. As a result, the according samples will remain certain mechanical strength needed in pervaporation.

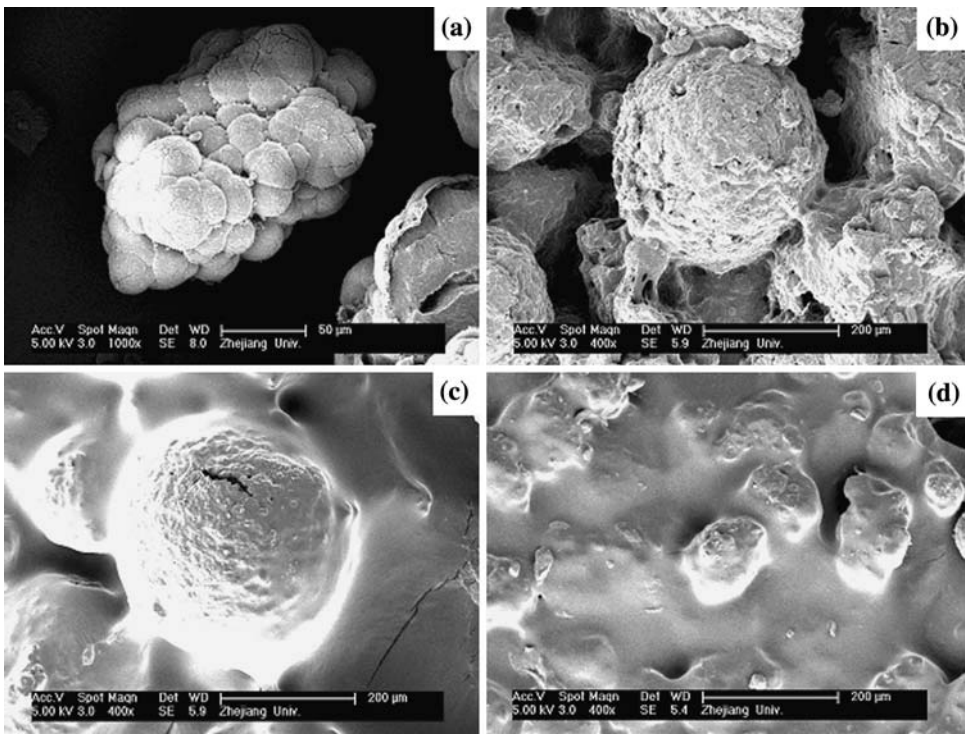

Fig. 5 SEM photographs of the products from copolymerization at different 1-octene concentrations. Samples a–d are in accordance with Table 1

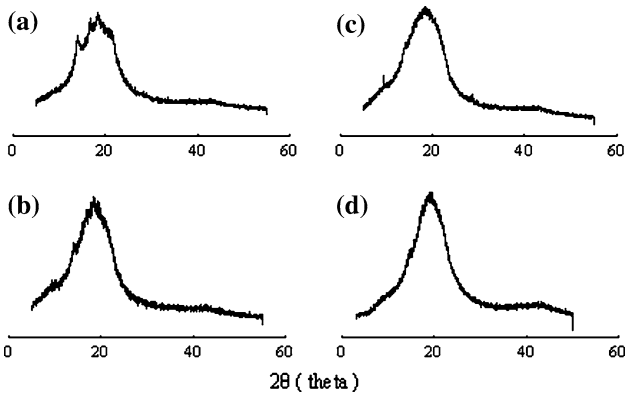

Fig. 6 WAXD patterns of P-*co*-Os with different compositions. Samples a–d are in accordance with Table 1

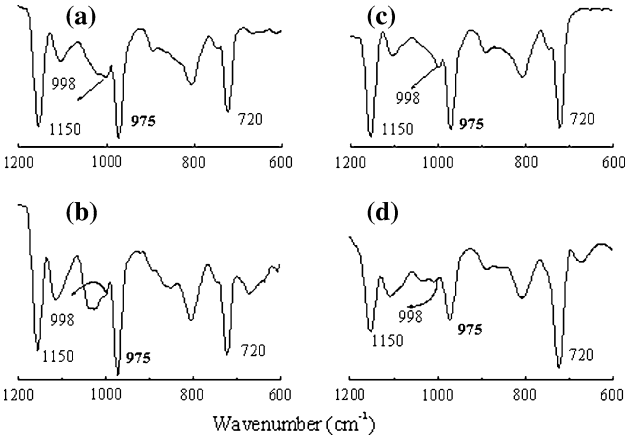

Fig. 7 FT-IR spectra of the P-*co*-Os with different compositions. Samples a–d are in accordance with Table 1

The thermal properties can be reflected by TGA analysis. The result is listed in Fig. 8. P-*co*-Os have excellent thermal stability since their weight loss starts at about 400 °C. This is one of the prerequisites for application of a given membrane in the pervaporation process.

Pervaporative properties of the P-*co*-Os coated PVDF/PET composite membranes

To improve the mechanical strength of the membrane and add up the permeate flux of the corresponding membrane, P-*co*-Os solutions are coated on the PET supported PVDF substrates. A comparison of the SEM microphotographs in Fig. 9(a, b) indicates that the coating layer is homogeneous and dense. In addition, Fig. 9(c) shows that small pore-penetration takes place, which is in favor of improving the permeate flux and guarantees a good combination between the skin layer and the substrate.

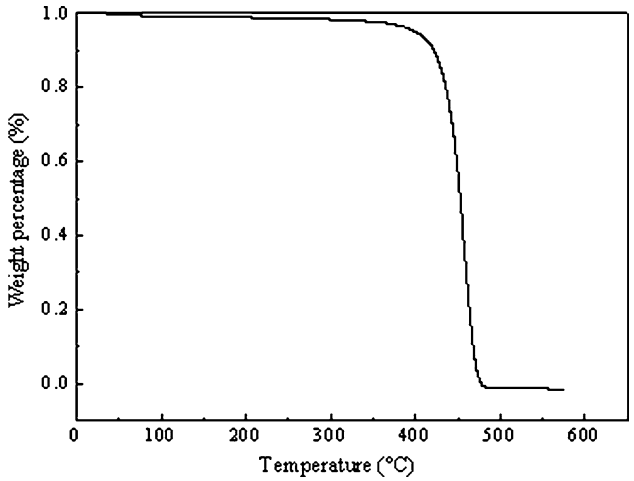

Fig. 8 TGA curve of P-*co*-Os with 24.6 mol% 1-octene content

The presence of crystalline phase in the polymeric matrix influences both the sorption of components into and their transport through the membrane [23]. All of the steps involved in the permeation process through a semi-crystalline polymer, namely sorption, diffusion, and desorption, take place in the amorphous region, whereas the crystal entities act as impermeable barriers. The penetrant molecules have to make a detour from the crystalline region and thus 'travel' a much longer distance through a semi-crystalline polymer than through a fully amorphous polymer. As a result, a decrease of the crystallinity to a lower degree will improve the diffusion through the polymeric matrix. This is proved by the pervaporation results in this article shown in Table 2. The permeate flux increases with increasing the 1-octene content in P-*co*-Os.

Table 2 also shows that each kind of copolymers (samples b–d) has a T_g between −50 °C and −30 °C. Therefore, they are in the rubbery state at room temperature, which implies the high permeation rate at medium temperature in pervaporation.

It should be noted that the premise for transport almost exclusively through the amorphous phase is conformational transitions which create voids for diffusion of the permeating molecules. So T_g is an important factor to characterize the permeation rate through a given polymer. As it is exhibited in Table 2, the lower T_g is the higher permeate flux appears. But the selectivity shows a reverse trend. That is, it decreases with a decrease of T_g. The reason can be narrated as follows. With 1-octene content in P-*co*-Os increasing, T_g of the relatively copolymer decreases, and amorphous regions are expanded and the macromolecular chains inside can move more easily. Thus both chloroform and water can diffuse easily in them because of more free volume, which contributes an increase of the permeate flux. Nevertheless, the rate of an increase in the water permeate

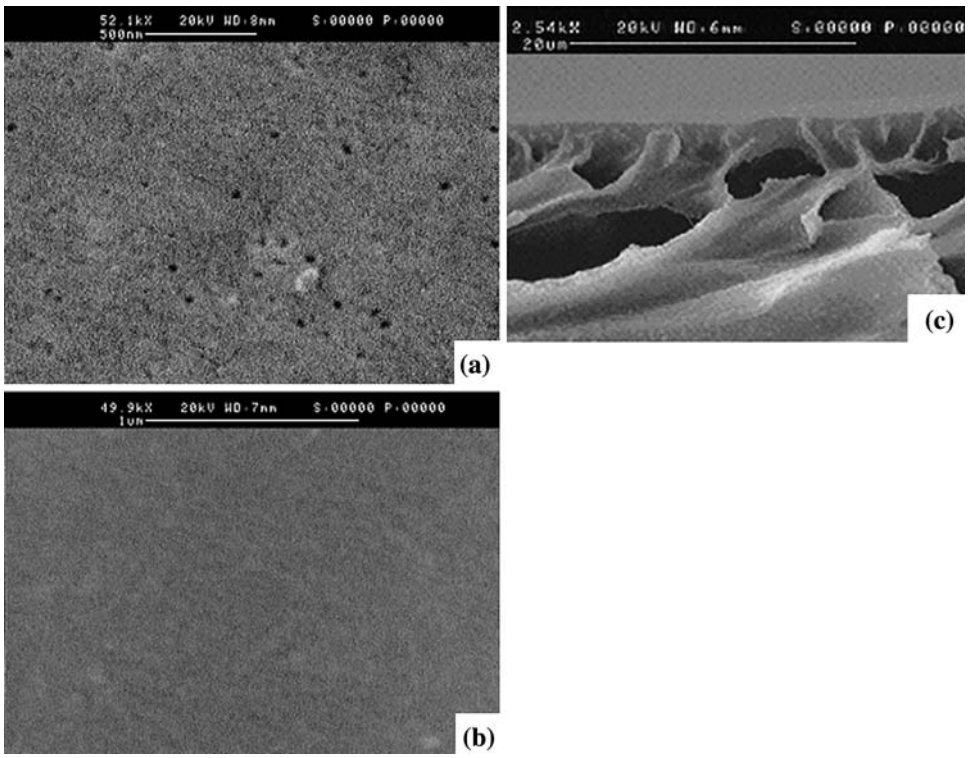

Fig. 9 SEM microphotographs of the membrane. (**a**) Surface of PVDF/PET supporting membrane; (**b**) surface of the P-*co*-Os coated PVDF/PET composite membrane; (**c**) cross-section of the P-*co*-Os coated PVDF/PET composite membrane

Table 2 The pervaporation properties of the P-*co*-Os coated PVDF/PET composite membranes with mean 5 μm thick active layer at 25 °C and 500 ppm chloroform concentration

P-*co*-Os samples	T_g (°C)	Permeate flux (10^3 kg/(m^2 h))		Separation factor α_{CHCl_3/H_2O}
		Chloroform	Water	
b	−33.5	22.3	40.1	1108
c	−36.8	30.6	56.9	1074
d	−41.5	41.1	88.8	927

flux is even higher than that in the chloroform permeate flux. As a result, the selectivity decreases.

In conclusion, it is not true that lower crystallinity results in better pervaporative separation properties. To assure high selectivity together with high permeate rate simultaneously, the content of 1-octene in P-*co*-Os should be in a certain range. Besides, to determine the optimal composition of P-*co*-Os, the condition employed during the copolymerization, such as the monomer concentrations, temperature, the kind of catalyst and its amount, etc. should be taken into account.

Conclusions

The binary sequence distribution of the synthesized P-*co*-Os and the average sequence lengths of propene and 1-octene indicate that 1-octene in the copolymeric backbone chains is mainly inlaid as an individual unit and the chain structures of the obtained copolymers are somewhat comb-like. Moreover, no homopolyoctene is admixed in the obtained copolymerization products.

In the case of the propene/1-octene copolymerization, the introduction of relatively long 1-octene branches will effectively reduce the crystal size and the crystallinity of the obtained P-*co*-Os. Under the condition employed in this article, and when the 1-octene concentration during copolymerization with propene is over 0.168 mol/L, the crystallinities of the obtained P-*co*-Os are positively low. FT-IR and WAXD analysis verify that the according P-*co*-Os are nearly amorphous and the crystals may exist in the form of crystallites.

P-*co*-Os have excellent thermal stability because the weight loss starts at about 400 °C during TGA tests. In addition, its break strength is higher than the generally used PDMS membrane in O-PV. That of P-*co*-Os with 1-octene content being 24.6 mol% is 1.7 MPa.

It is demonstrated that P-*co*-Os exhibit prospects for O-PV. An increase of 1-octene content in P-*co*-Os results in a decrease of T_g, and the higher permeate flux appears. But simultaneously the selectivity shows a decreasing trend. To assure high selectivity with high permeate rate, the content of 1-octene in P-*co*-Os should be in a certain range and determined combining the condition employed during the copolymerization, such as the monomer concentrations, temperature, the kind of catalyst and its amount, and so on.

Acknowledgements This article was supported by the National Natural Science Foundation of China (No. 20704018), the Open Project Program of Key Laboratory of Eco-Textiles, Ministry of Education, China (No. KLET0612) and the Natural Science Initial Research Foundation of Jiangnan University (No. 206000-52210671).

References

1. Peng M, Vane LM, Liu SX (2003) J Hazard Mater 98(1–3):69
2. Lipnizki F, Hausmanns S, Ten P-K, Field RW, Laufenberg G (1999) Chem Eng J 73(2):113
3. Feng X, Huang RYM (1997) Ind Eng Chem Res 36(4):1048
4. Ten RK, Field RW (2000) Chem Eng J 55(8):1425
5. Wijmans JG, Baker RW (1995) J Membr Sci 107(1–2):1
6. Wijmans JG (2004) J Membr Sci 237(1–2):39
7. Schaetzel P, Vauclair C, Nguyen QT, Bouzerar NJ (2004) J Membr Sci 244(1–2):117
8. Schaetzel P, Vauclair C, Luo G, Nguyen QT (2001) J Membr Sci 191(1–2):103
9. Peng M, Vane LM, Liu SX (2003) J Hazard Mater 98:69
10. Han S, Puech L, Law RV, Steinke JHG, Livingston A (2002) J Membr Sci 19(1–2):1
11. Bell CM, Gerner FJ, Strathmann H (1988) J Membr Sci 36:315
12. Pereira CC, Rufino JRM, Habert AC, Nobrega R, Cabral LMC, Borges CP (2005) J Food Eng 66(1):77
13. Nijhuis HH, Mulder MHV, Smolders CA (1993) J Appl Polym Sci 47(12):2227
14. Xu ZK, Feng LX, Wang DL, Yang SL (1991) Die Makromolekulare Chemie 192(8):1835
15. Tian XZ, Zhu BK, Jiang X, Xu YY (2005) Chinese J Polym Sci 23(6):623
16. Fu Z, Xu J, Zhang Y, Fan Z (2005) J Appl Polym Sci 97(2):640
17. Tian X, Zhu B, Xu Y (2005) J Membr Sci 248(1–2):109
18. Lovisi H, Tavares MIB, Silva NM, Menezes SMC, Maria LCS, Coutinho FBC (2001) Polymer 42(24):9791
19. Yan D, Wang W-J, Zhu S (1999) Polymer 40(7):1737
20. Meng LZ, Gong SL, He YB (2003) Analysis of organic spectrum. Wuhan, Wuhan University Publishing House, China, p 144
21. Shen D (1982) Application of FTIR methods in macromolecular research. Beijing, Scientific Publishing House, China
22. Li L, Xiao Z, Zhang Z, Tan S (2004) Chem Eng J 97(1):83
23. Long RB (1965) Ind Eng Chem Res 4:445